

A Small Form Factor Impedance Tuned Microstrip Antenna with Improved Gain Response

Seshadri Binaya Behera, Debaprasad Barad*, and Subhrakanta Behera

Abstract—This research work adopts an open-circuited-series stub-tuning in sequence with unmatched antenna radiator to bring out a small form factor. Thereby, the effective antenna radiator size has been shrunk up to 0.2λ , where similar efficiency and beam pattern has been maintained. The antenna is conceptualized with symmetrical slots, which indicates a multi-ring structure to contribute multiband miniaturization. This consists a loop based rectangular-ring connected with an E-shaped patch, which is excited through a microstrip stepper impedance transmission line followed by an equally distributed strip-line. It enables enhanced impedance-matching at 2.76 GHz and 6.34 GHz by a stepper impedance transmission line with stub-loading technique. The antenna aperture area miniaturization of 56% has been achieved by introducing slots on the radiator patch. Moreover, this miniaturized patch exhibits improved gain response of 4.43 dBi and 5.37 dBi in the broadside direction. The proposed design occupies a dimension of $(0.22\lambda \times 0.26\lambda)$ mm².

1. INTRODUCTION

Present-day communication system employs compact wireless devices to meet the requirement of proliferating wireless technology. To confront all the requirements of the modern technology, microstrip patch antennas (MSA) are the ultimate candidates as of the authors' best knowledge, for the exceptional features, such as low cost, low profile, low weight, and ease of fabrication. Furthermore, it is absolutely desirable to adopt multi-standard compact devices. This necessitates meticulous investigations on 'patch miniaturization'. The miniaturization techniques provide flexibility in designing small form factor (SFF) patch antennas to acquire low frequency operations without going for large dimensions. Here, it should be mentioned that any design that is physically smaller than the other similar designs of the domain can be considered to be of small form factor. Over the last decade, many research insights have been put into miniaturization of patch antennas [1–21].

An antenna with low loss barium titanate ceramic composite material, with very high dielectric constant is investigated in [3] for size reduction. But the high dielectric contrast between the substrate and air gives rise to surface waves, which degrades the antenna performance. A study in [4] shows miniaturization using Defected Microstrip Structure (DMS). Fractal [5] is a very popular technique for patch miniaturization, and the percentage of size reduction is proportionate to the fractal iterations. Fractal techniques combined with meta-material is reported in [6]. A DGS hexagonal compact patch antenna with six triangular slots cut on the ground plane exactly below the corners of the radiator patch has been reported for making the patch compact in [7]. Another dual-band defected ground structure is investigated in [8] with a stacked configuration, and 36% of compactness has been observed. Shorting wall [9, 10] and shorting pins [11] are also very useful techniques for patch size reduction. A design with four L-shaped shorting strips is proposed in [12] to reduce the patch size. A semicircle arc projection method using nonuniform patches has been employed in [13] to effectively reduce the

Received 19 March 2020, Accepted 9 July 2020, Scheduled 3 August 2020

* Corresponding author: Debaprasad Barad (deba7482@gmail.com).

The authors are with the KIIT University, India.

patch size. High level of miniaturization can be realized by adding a metamaterial-inspired layer [14] in between the ground plane and radiator patch layer without affecting the radiation efficiency of the patch. The use of metamaterial structures [15, 16] to obtain size reduction can be found in the literature. Even though these miniaturization techniques contribute to size reduction of the patch antenna, on the other hand it degrades the antenna performance in terms of gain and efficiency. Likewise, some modern techniques have been experimented to realize the miniaturization using a TL-MTM structure [17], stepped impedance transformer [18], and DRA on a C-slot based structure [19]. However, these antennas show good bandwidth where it loses gain and vice-versa. Miniaturized ring patch antennas have been considered in [20, 21], and it is shown that ohmic loss reduction plays an essential role for gain enhancement. A portion of the central part of a patch is cut in [22] to improve gain. Also, effects of slots on a patch are studied in [23, 24] which claim that the slots can be used as an efficient technique to attain miniaturization. This research aims to achieve higher miniaturization by implementing a slotted radiating aperture which can also lead to gain enhancement.

This work investigates a compact slotted patch antenna to realize maximum possible miniaturization. Here, the small form factor patch has been developed by integrating the combination of stub and slot loading techniques onto the antenna aperture. The proposed antenna is excited through a transmission line feeding with a symmetric open circuited series stub matching. This structure can be viewed as an inset-fed microstrip patch shaped into a split-ring-like structure while enclosing a dumbbell shaped patch, which later gets engraved with rectangular slots. With this configuration the antenna realizes a dual-band characteristic. To improve the impedance matching at the resonances, symmetrical stubs have been loaded on a transmission line. The stub tuned configuration exhibits good return losses of 19 and 16 dB at 2.76 GHz and 6.34 GHz, respectively. This antenna can find its applications in NEXRAD (Next Generation Weather Radar) systems operated by the National Weather Service (NWS) in the band 2700–2900 MHz [25] and for long-distance radio telecommunications i.e., C-band applications. Typically, miniaturization with small form factor degrades the gain of the antenna [26]; however, the insertion of slots over the dumbbell-shaped patch enhanced the radiation characteristics and improved the gain at both resonances. Moreover, the proposed dual-band compact patch contributes a new design technique which can be realized from the transparent design flow and Table 1.

Table 1. Performance comparison of various miniaturization techniques.

Ref.	Antenna Size	Resonances	Techniques	Gain (dBi)
This Work	$21 \times 17 \times 1.6 \text{ mm}^3$	2.76 GHz, 6.34 GHz	Split ring slotted configuration	4.43, 5.37
[17]	$36 \times 36 \times 3 \text{ mm}^3$	2.76 GHz, 5.23 GHz	TL-MTM Structures	1.02, 6.8
[16]	$64 \times 45 \times 1 \text{ mm}^3$	2.5 GHz, 5.8 GHz	Stepped Impedance resonator	-1.8, 1.1
[19]	$40 \times 40 \times 4.9 \text{ mm}^3$	2.5 GHz, 5.8 GHz	Dielectric resonator antenna (DRA) using a parasitic c-slot	4.3, 3.8
[28]	$170 \times 170 \times 0.8 \text{ mm}^3$	2.45 GHz, 5.3 GHz	Circular Ring and a Concentric Disk with multi-mode configuration	6.06, 3.4

The paper is structured into four parts to give a better representation of the proposed work. The design and parametric analysis of the proposed work are discussed in Section 2. The antenna performance is validated through experimental analysis and discussed in Section 3. At last, the research work is summarized in Section 4.

2. PROPOSED COMPACT ANTENNA CONFIGURATION

The proposed compact antenna is designed on a low cost FR4 substrate of dielectric constant $\epsilon_r = 4.4$, thickness $h_1 = 1.6 \text{ mm}$, $\tan \delta = 0.02$. The proposed antenna initiator includes a rectangular patch with an inset-fed microstrip transmission line feed for excitation. The designed feed is connected to a 50-ohm SMA connector.

2.1. Configuration of Basic Miniaturization Antenna patch

The patch antenna is designed with an FR4 substrate of height 1.57 mm and dielectric constant 4.4. Initially, an inset-fed patch of $(17 \times 21) \text{ mm}^2$ without any irregularity was taken into consideration, which is later remodeled into a split-ring-like structure enclosing a dumbbell shaped patch (Antenna 2). This has been realized by loading two psi-shaped slots along both the radiating edges of the patch. The vertical gaps are maintained between the two E-shaped patches, $G_e = 3 \text{ mm}$, and the width of the E-patch, $W_e = 2.5 \text{ mm}$. Again, two symmetrical rectangular slots are etched out of the dumbbell-shaped patch to achieve miniaturization. Like so, the radiating patch (Antenna 3) gets an impression of two E-shaped patches enclosing another two rectangular metallic rings, which are connected through a stripline, and it is centrally excited by an inset-fed line. The width of the rectangular rings, $W_r = 0.5 \text{ mm}$; the horizontal distance between the E-shaped patch and the rectangular ring patch, $G_{er} = 1.5 \text{ mm}$. To maintain a physical continuity on the patch surface, three connecting patches are formed on the proposed structure, and its dimensions are denoted by $W_1 = L_1 = 3 \text{ mm}$ and $W_2 = L_2 = 1.5 \text{ mm}$, in Figure 1.

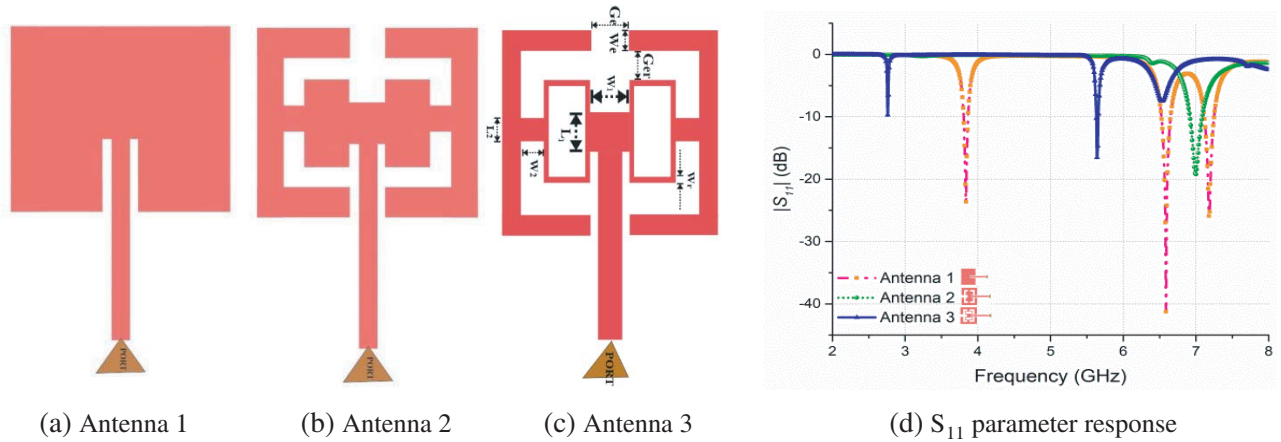


Figure 1. Structure of the proposed miniaturized patch and its S_{11} response.

The basic concept behind miniaturization is to increase the electrical path-length of current flow on the surface of the radiating aperture. By inserting slots on the patch surface, the existing path of current flow can be disturbed, and the current flow direction can be forced to meander. This may result into a longer current flow path, thus enabling the patch to resonate over a lower frequency. With this approach, a set of slots, after analyzing the surface current distribution, are loaded on the radiator patch which creates a loop path and increases the current path in the designed geometry. The variations in the resonance behavior of the patch are due to the slots as depicted in Figure 1(d). Though the 1st set of slots excite the patch at a higher frequency, the combination of both sets of slots enable the patch to resonate at a lower frequency. The patch which was supposed to resonate over 3.78 GHz now resonates at 2.76 GHz after miniaturization. Also, the slots enhance resonance characteristics of the patch to multiband operation.

From [25], it is evident that a microstrip patch of dimension nearly $(26 \times 33) \text{ mm}^2$ resonates at 2.76 GHz, whereas this work is realized with a dimension of $(17 \times 21) \text{ mm}^2$, while introducing slots in the aperture. Hence, adding slots realizes effective miniaturization and demonstrates size reduction of the microstrip antenna. According to Chu’s limit [27], the minimum Q limit of a small linearly polarized antenna can be characterized by

$$Q = \frac{1}{k^3 a^3} + \frac{1}{ka} \tag{1}$$

where $k = 2\pi/\lambda$, λ is the operating wavelength, and ‘ a ’ is the radius of the smallest possible sphere which the antenna can fit into. For an electrically small antenna, (ka) should be less than 1. The (ka) value at the first resonance is 0.831, thus justifying the antenna miniaturization.

The quality factor of the antenna can be computed from the relative bandwidth. Since the impedance bandwidth of the antenna is very narrow, it can be considered as a high-Q antenna (i.e., the 1st resonance is 2753 MHz–2773 MHz; quality factor is 139 and at the 2nd resonance 6302 MHz–6381 MHz; quality factor is 81). High Q antennas are well suited for receiver application as it can filter out signals which are ‘out-of-band’.

As the ohmic losses of a microstrip patch increases after miniaturization, the radiation characteristics gain and efficiency decrease significantly [27]. Figure 2 shows that the reflection-coefficient degrades after miniaturization.

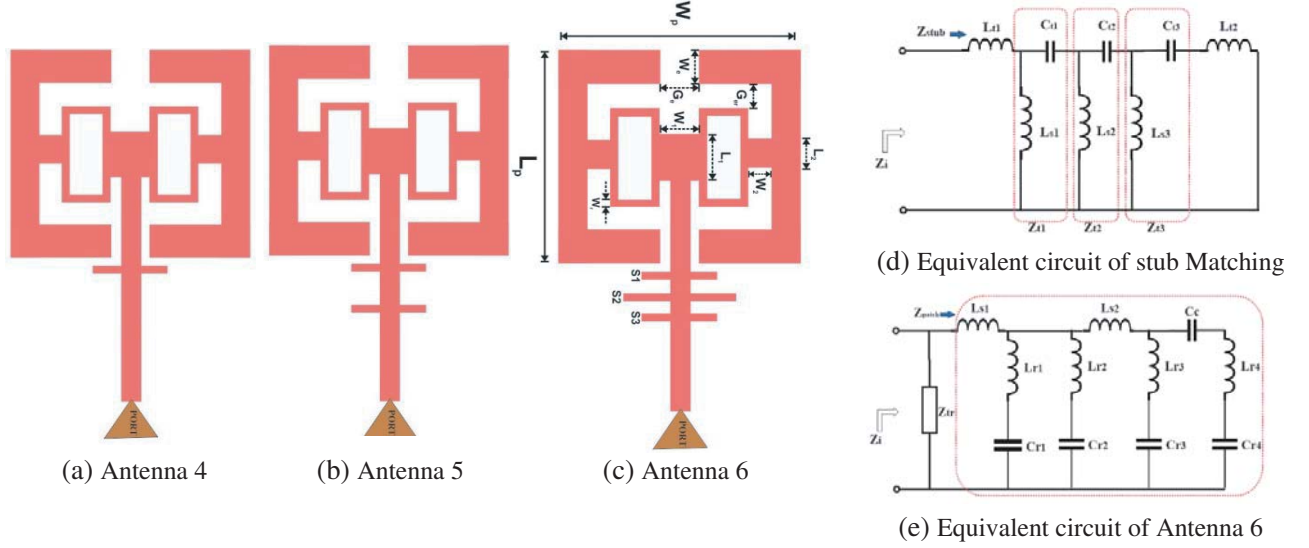


Figure 2. Design of irregular transmission line feed.

2.2. Stub Matched Impedance Transformation

In theoretical aspects, miniaturization degrades the matching profile of the antenna; hence to confirm acceptable impedance matching stub-matching technique has been investigated using single stub (antenna 4), double stub (antenna 5) and concluded with stub matching design (antenna 6). The feed line of length 20.25 mm is hefted with three symmetrical stubs, denoted as $S1$, $S2$, and $S3$, and thus the final layout of Antenna 6 has been acquired. The distance of the first stub $S1$ from its nearest patch edge $Sd = 0.5$ mm. Width of $S1 =$ width of $S2 =$ width of $S3 = 1$ mm. Length of $S1 =$ Length of $S3 = 7$ mm, and Length of $S2 = 11$ mm. Figure 2 illustrates the design evolution of the antenna structure with matching stubs.

The sequential stub-loading improves the matching performance by the additional inductance and capacitance offered by each stub. Here, the open-circuit-series-stub tuned transmission line (Figure 2(d)) along with the antenna (Figure 2(e)) is replaced with equivalent inductance (L) and capacitance (C) where the surface resistance can be ignored for high frequency analysis. The illustrated lumped circuit equivalent of the stepped impedance transformer is analyzed based on the current flow and electric field accumulation due to microstrip discontinuity. The three-stage stub loading forms a connected T-junction which influences charge accumulation near each T-Junction. The electric field accumulation can be represented as $L_{s1} \parallel C_{t1} \dots L_{s3} \parallel C_{t3}$.

Impedance stub-loaded transmission line can be calculated;

$$Z_{tr} = j\omega L_{t1} + Z_{t1} + Z_{t2} + Z_{t3} + j\omega L_{t2} \quad (2)$$

where Z_{t1} , Z_{t2} , and Z_{t3} are the equivalent impedance offered by each T-junction, which can be determined as below;

$$Z_{t1} = j\omega L_{s1} \parallel \frac{1}{j\omega C_{t1}} = \frac{L_{s1}}{j\omega C_{t1} \left(L_{s1} - \frac{1}{\omega^2 C_{t1}} \right)} \quad (3)$$

$$Z_{t2} = j\omega L_{s2} \parallel \frac{1}{j\omega C_{t2}} = \frac{L_{s2}}{j\omega C_{t2} \left(L_{s2} - \frac{1}{\omega^2 C_{t2}} \right)} \quad (4)$$

$$Z_{t3} = j\omega L_{s3} \parallel \frac{1}{j\omega C_{t3}} = \frac{L_{s3}}{j\omega C_{t3} \left(L_{s3} - \frac{1}{\omega^2 C_{t3}} \right)} \quad (5)$$

In Figure 2(e), the patch is represented as a rectangular ring which is represented as series inductance (L_{r1} and L_{r2}) and capacitance (C_{r1} and C_{r2}) whereas the E-shaped patches are represented as series inductance (L_{r3} and L_{r4}) and capacitance (C_{r3} and C_{r4}) separated by a capacitance C_c . The net input impedance (Z_i) can be realized by considering the feed line impedance (Z_{tr}) and radiating patch impedance (Z_{patch}). The impedance can be reevaluated as

$$Z_i = \frac{Z_{tr} Z_{patch}}{Z_{tr} + Z_{patch}}$$

Equation (6) relates the input impedance (Z_i) to the stub-loaded feed line (Z_{tr}) which controls the reflection coefficient parameter with a known characteristic impedance. This states that the impedance tuning by stub-loading yields better impedance matching than a conventional transmission line, which can be observed from Figure 3. It shows that the impedance matching characteristics are enhanced without altering the resonance behavior of the patch at the first resonance, whereas Antenna 6 yields better return loss characteristics at the second resonance, i.e., 6.34 GHz. Hence, it can be realized that the addition of stubs contributes to a better return loss at the first resonance, though it makes the return loss properties at the second resonance a little worse.

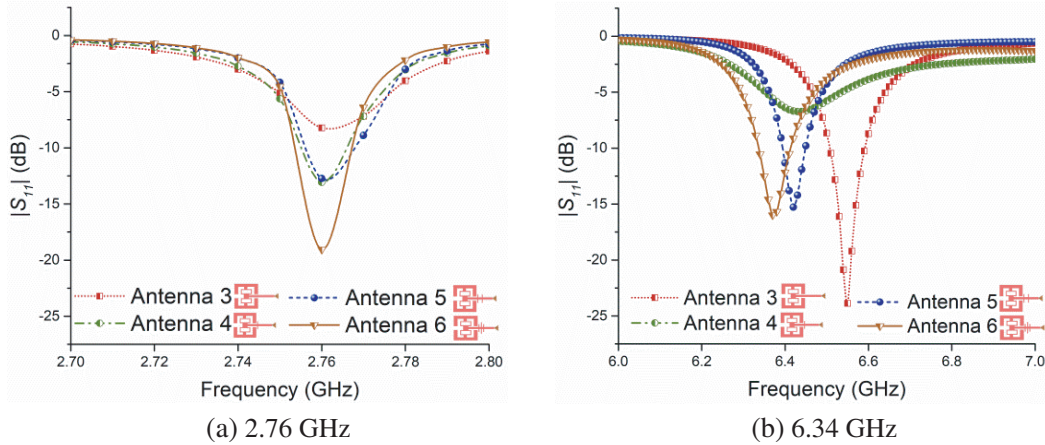


Figure 3. S_{11} parameters of the patch with stepped impedance transformer.

The position of the three stubs are varied on the feed line, and it is observed that the closer the stubs to the radiator patch are, the better the antenna performance is in terms of return loss. This variation is portrayed in Figure 4. Here, the distance between the first stub $S1$ and the radiator patch edge Sd is varied while keeping the distances in between the three stubs the same.

2.3. Analysis of Proposed Miniaturized Antenna

The rectangular slots imposed on the central-upper and lower halves of the patch create two metallic rings on it. A parametric study on the effect of the ring-width on return loss characteristics has been carried out and is illustrated in Figure 5. It can be observed that a slender metallic ring yields better performance at the first resonance, in terms of return loss, than a wide ring patch.

The field distribution of the electrically small antenna is varied in accordance with the insertion of slots in the aperture, and the E -field concentration is denser with the introduction slots and stub

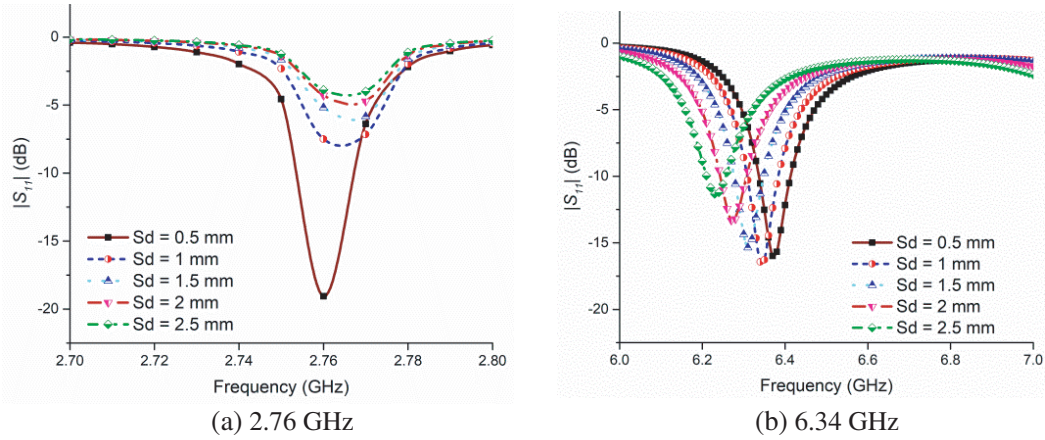


Figure 4. Variation of position of the stubs along the feed line.

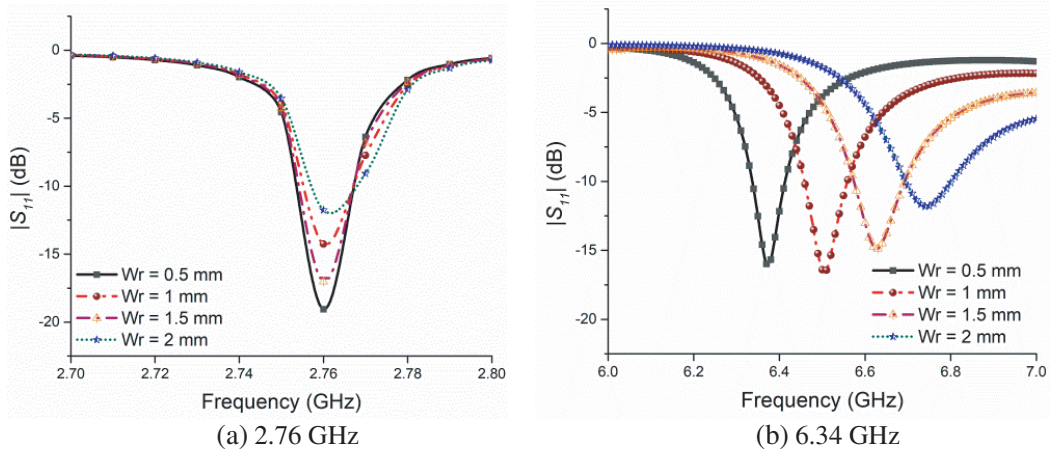


Figure 5. S_{11} responses of the proposed structure with different metallic ring-widths.

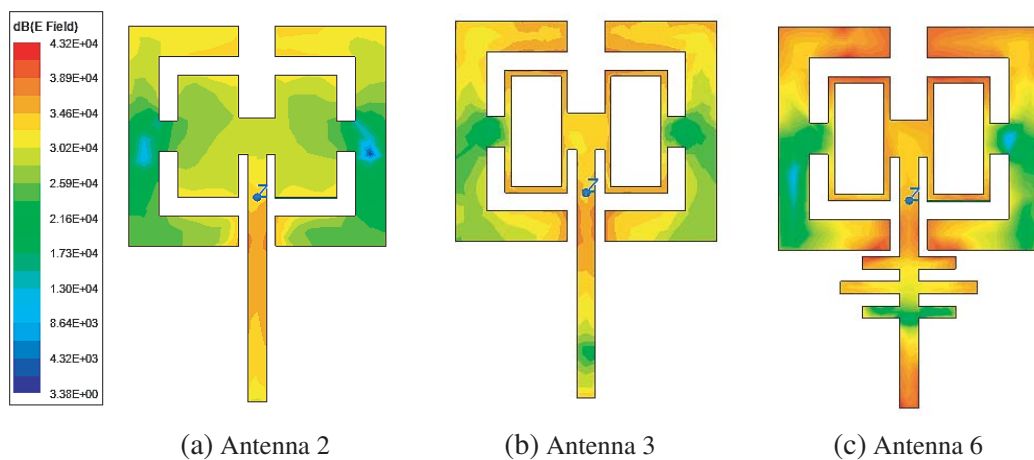


Figure 6. Field distribution at different configuration.

matching as shown in Figure 6. From this it can be assumed that the maximum illumination occurs in antenna 6 which directs the maximum radiation towards the broadside direction, thus leading to gain improvement. The variation of gain with respect to frequency for three different antenna configurations

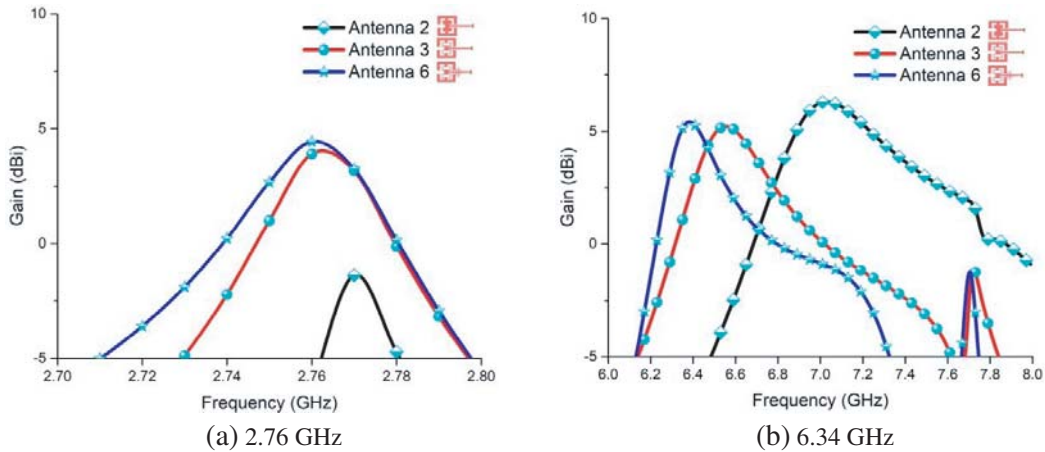


Figure 7. Simulated gain response of the proposed antenna with different configurations.

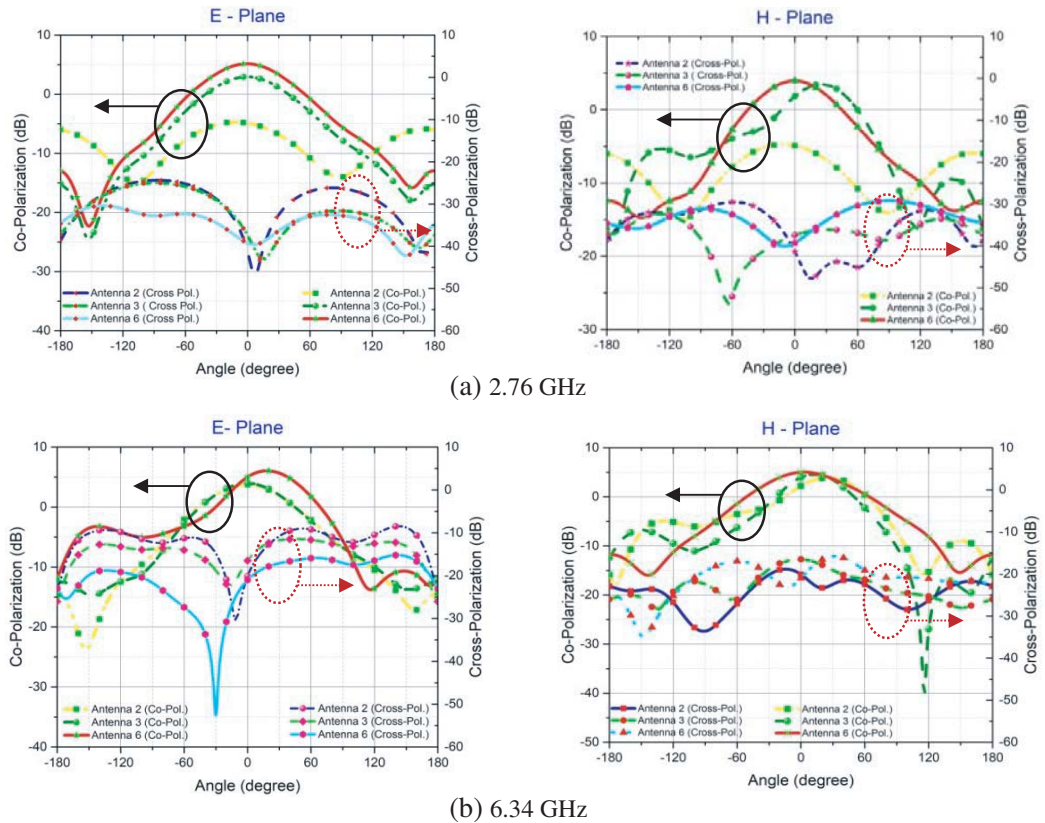


Figure 8. Simulation radiation pattern with different antenna configuration.

has been laid out in Figure 7.

The simulated patterns of the proposed slotted antenna are acquired for each design iteration using HFSS EM suite which show a significant improvement from one to another configuration. The acquired radiation patterns are plotted in cartesian graph for clear demonstration of parametric enhancement as illustrated in Figure 8. Both the co-polarization and cross-polarization patterns are observed at both *E*- and *H*-planes as illustrated in the same figure. The parametric study concludes that the slots in antenna 6 with perfect impedance matching potentially forms a symmetric broadside beam which leads to delivering an improved gain response.

3. SIMULATION AND MEASURED RESULTS

The designed structure has been fabricated on an FR4 dielectric substrate with dielectric constant 4.4, substrate height 1.57 mm, and tangent loss 0.02. This structure has been developed using a photolithography process, and proper alignment has been carried out during fabrication process to avoid the tolerance in testing results. An SMA connector is connected to the microstrip feed line to provide sufficient electromagnetic excitation. The fabricated microstrip patch is of dimension 18 mm \times 21 mm \times 1.57 mm. The fabricated prototype of the proposed miniaturized slotted antenna with a stepped impedance transformer is illustrated in Figure 9(a). The simulated and measured return loss characteristics are shown in Figure 9(b), from which it can be observed that there is a slight difference (minimum tolerance) in measured and simulated results at the first resonance. This difference can be explained as an outcome of fabrication error, the SMA connector, and the numerical error. At the second resonance, due to better matching effect the return loss is improved to 21.79 dB.

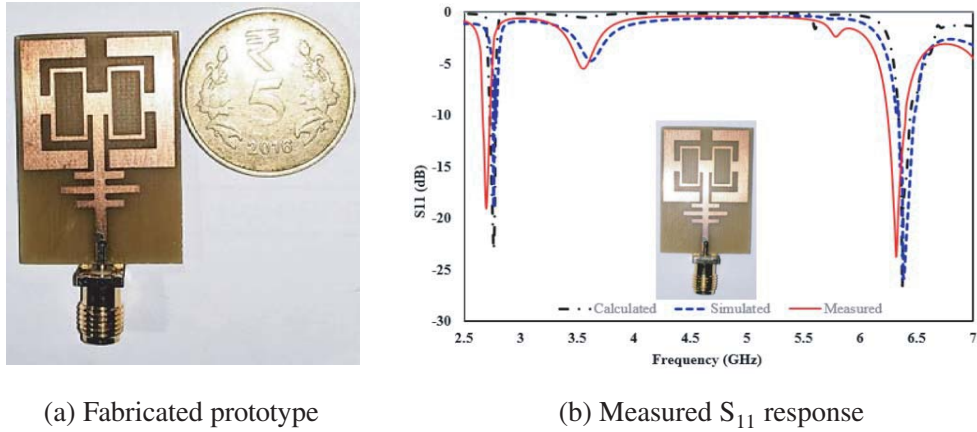


Figure 9. Fabricated prototype of proposed CPMA and its S_{11} response.

Measurement of the antenna structure was carried out in a microwave anechoic chamber without a large metal plate as its ground plane, and gain response of the fabricated prototype has been determined by using the reference standard horn procedure inside the anechoic chamber. As the structure exhibits dual-band characteristics, the gain and radiation patterns obtained over both the resonances are nearly same. The simulated and measured radiation patterns agree well with each other. The measured radiation patterns are plotted and shown in Figure 10. At both the planes, the back-radiation levels at both the resonances are within the acceptable limit, and it is caused as the ground plane used is not sufficient to block the back radiation. Also it can be observed that the F/B ratio (Front to Back Ratio) is roughly around 10 dB, which falls under the acceptable limit.

Furthermore, the radiation efficiency of the proposed antenna has been observed and plotted in Figure 11 along with the VSWR response. The antenna shows good efficiency at both the resonances, and a good VSWR of 1.5:1 is also achieved with the stub matched investigation as shown in the same figure.

Table 2. Antenna performance.

Resonant Frequency (GHz)	Return Loss (dB)		Gain (dBi)	
	<i>Simulated</i>	<i>Measured</i>	<i>Simulated</i>	<i>Measured</i>
2.76	19	17.2	4.43	4.18
6.34	16	21.19	5.37	5.05

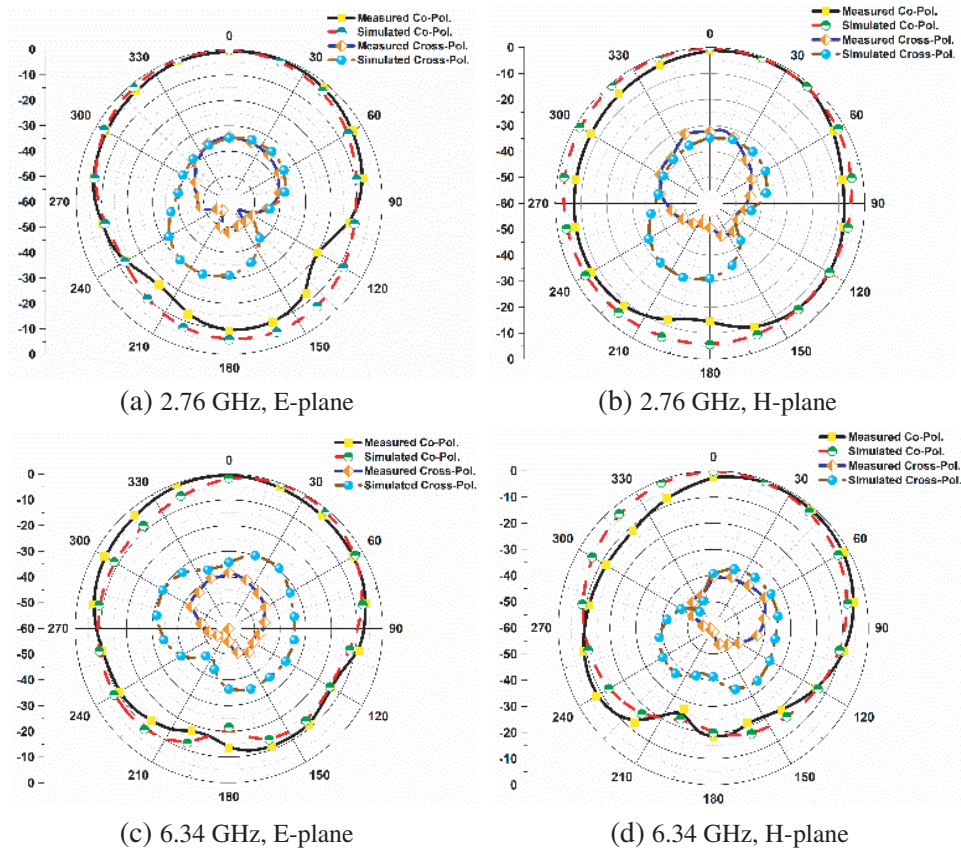


Figure 10. Simulated and measured Radiation Pattern of the proposed antenna.

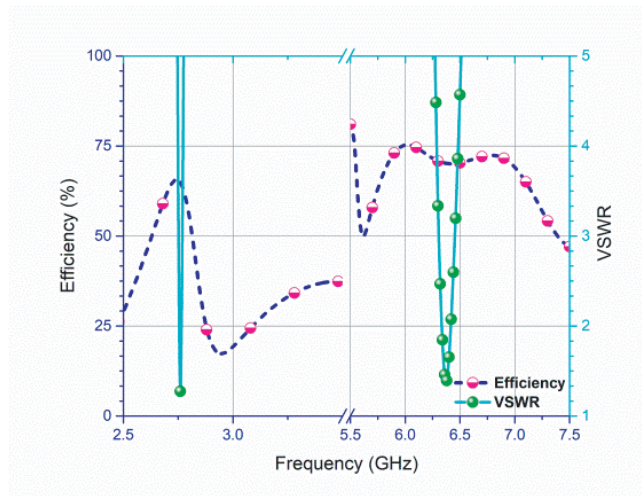


Figure 11. Efficiency and VSWR of the proposed antenna.

The antenna performance results obtained during simulation and experiment have been summarized in Table 2. The measured return loss at the first resonance is nearly equal to the simulation result. The slight variation between simulated and measured results might be caused by the fabrication error. At the second resonance, though simulated gain response is better than measured gain, measured return loss is much better than simulated result due to better matching effect. Similarly, a slight improvement in bandwidth can be observed at the second resonance.

4. CONCLUSION

An electrically small antenna has been proposed by using slots. The effective aperture size of the antenna radiator has been shrunk up to 0.2λ which brings out a small form factor. This antenna yields a dual-band response at 2.76 GHz and 6.34 GHz with return loss bandwidths of 20 MHz and 79 MHz, respectively. The overall gain response of the patch is better than 4.2 dBi which was around 0 dBi at the beginning. Return loss improvement has been achieved by open-circuited-series stub-tuning on the transmission feed. The lowest resonance shifts back to 2.76 GHz from 3.78 GHz by adding slots, and thus around 31% of frequency miniaturization and an overall size reduction by 56% have been achieved. It can also be concluded that the insertion of slots boosts the current concentration encircling the slots, thus affecting the radiation characteristics of the patch, and the positions of the slots affect the resonance behavior of the patch.

REFERENCES

1. Biswas, P., S. De, B. Bag, D. Chanda Sarkar, S. Biswas, and P. P. Sarkar, "Dual ISM band printed antenna with omnidirectional radiation pattern and better radiation efficiency," *Int. J. RF Microw. Comput. Aided Eng.*, Vol. 29, e21780, 2019.
2. Singh, A. K., M. P. Abegaonkar, and S. K. Koul, "Miniaturized multiband microstrip patch antenna using metamaterial loading for wireless application," *Progress In Electromagnetics Research C*, Vol. 83, 71–82, 2018.
3. Zhang, Y. P., "A dielectric loaded miniature antenna for microcellular and personal communication," *Proc. IEEE AP-Symp.*, 1152–1155, June 1995.
4. Hanae, E., N. Amar Touhami, and M. Aghoutane, "Miniaturized microstrip patch antenna with spiral defected microstrip structure," *Progress In Electromagnetics Research Letters*, Vol. 53, 37–44, 2015.
5. Hung, T., J. Liu, C. Wei, C. Chen, and S. Bor, "Dual-band circularly polarized aperture-coupled stack antenna with fractal patch for WLAN and WiMAX applications," *Int. J. RF Microw. Comput. Aided Eng.*, Vol. 24, 130–138, 2014.
6. Samantaray, D., S. Bhattacharyya, and K. V. Srinivas, "A modified fractal-shaped slotted patch antenna with defected ground using metasurface for dual band applications," *Int. J. RF Microw. Comput. Aided Eng.*, Vol. 29, e21932, 2019.
7. Mandal, K. and P. P. Sarkar, "A compact high gain microstrip antenna for wireless applications," *AEU International Journal of Electronics and Communication*, Vol. 67, 1010–1014, 2013.
8. Khandelwala, M. K., B. K. Kanaujia, S. Dwaria, S. Kumar, and A. K. Gautam, "Analysis and design of dual band compact stacked Microstrip patch antenna with defected ground structure for WLAN/WiMax applications," *AEU International Journal of Electronics and Communication*, Vol. 69, 39–47, 2015.
9. Pinhas, S. and S. Shtrikman, "Comparison between computed and measured bandwidth of quarter-wave microstrip radiators," *IEEE Trans. Antennas and Propag.*, Vol. 36, No. 11, 1615–1616, November 1988.
10. Chair, R., K. F. Lee, and K. M. Luk, "Bandwidth and cross-polarization characteristics of quarter-wave shorted patch antennas," *Microw. Opt. Technol. Lett.*, Vol. 22, No. 2, 101–103, 1999.
11. Waterhouse, R., "Small microstrip patch antenna," *Electron. Lett.*, Vol. 31, No. 8, 604–605, 1995.
12. Shi, H., J. Li, J. Shi, J. Chen, Z. Li, S. Zhu, T. A. Khan, and A. Zhang, "Miniaturized circularly polarized patch antenna using coupled shorting strip and capacitive probe feed," *AEU International Journal of Electronics and Communication*, Vol. 98, 235–240, 2019.
13. Motevasselian, A. and W. G. Whittow, "Miniaturization of a circular patch microstrip antenna using an arc projection," *IEEE Antennas & Wireless Propagation Letters*, Vol. 16, 517–520, 2017.
14. Ouedraogo, R. O., E. J. Rothwell, A. R. Diaz, K. Fuchi, and A. Temme, "Miniaturization of patch antennas using a metamaterial-inspired technique," *IEEE Trans. Antennas and Propag.*, Vol. 60, No. 5, 2175–2182, 2012.

15. Jahani, S., J. Rashed-Mohassel, and M. Shahabadi, "Miniaturization of circular patch antennas using MNG metamaterials," *IEEE Antennas & Wireless Propagation Letters*, Vol. 9, 1194–1196, 2010.
16. Farzami, F., K. Forooraghi, and M. Norooziarab, "Miniaturization of a microstrip antenna using a compact and thin magneto-dielectric substrate," *IEEE Antennas & Wireless Propagation Letters*, Vol. 10, 1540–1542, 2011.
17. Zong, B., G. Wang, C. Zhou, and Y. Wang, "Compact low-profile dual-band patch antenna using novel TL-MTM structures," *IEEE Antennas & Wireless Propagation Letters*, Vol. 14, 567–570, 2015.
18. Hsieh, C., C. Wu, and T. Ma, "A compact dual-band filtering patch antenna using step impedance resonators," *IEEE Antennas & Wireless Propagation Letters*, Vol. 14, 1056–1059, 2015.
19. Chen, H., Y. Wang, Y. Lin, S. Lin, and S. Pan, "A compact dual-band dielectric resonator antenna using a parasitic slot," *IEEE Antennas & Wireless Propagation Letters*, Vol. 8, 173–176, 2009.
20. Hanae, E., N. Amar Touhami, M. Aghoutane, S. El Amrani, A. Tazón, and M. Boussouis, "Miniaturized microstrip patch antenna with defected ground structure," *Progress In Electromagnetics Research C*, Vol. 55, 25–33, 2014.
21. Latif, S. I., L. Shafai, and C. Shafai, "An engineered conductor for gain and efficiency improvement of miniaturized microstrip antennas," *IEEE Antennas Propag. Mag.*, Vol. 55, No. 2, 77–90, 2013.
22. Luo, Y. and Z. N. Chen, "A gain-enhanced patch antenna using a ghost reversal source," *Proc. in IEEE International Workshop on Antenna Technology (iWAT)*, 1–4, China, 2018.
23. Ambresh, P. A., P. M. Hadalgi, P. V. Hunagund, "Effect of slots on microstrip patch antenna characteristics," *2011 International Conference on Computer, Communication and Electrical Technology (ICCCET)*, 239–241, March 18–19, 2011.
24. Ansari, J. A., A. Mishra, N. P. Yadav, P. Singh, and B. R. Vishvakarma, "Analysis of W-slot loaded patch antenna for dualband operation," *AEU International Journal of Electronics and Communication*, Vol. 66, 32–38, 2012.
25. www.ntia.doc.gov/files/ntia/publications/compendium.
26. Balanis, C. A., *Antenna Theory Analysis and Design*, 3rd Edition, A John Wiley & Sons, INC Publication, 2003.
27. Chu, L. J., "Physical limitations of omni-directional antennas," *Journal of Applied Physics*, Vol. 19, 1163–1175, 1948.
28. Gan, B., L. Zhou, Y. Zhang, and J. Mao, "A dual-band microstrip antenna using a circular ring and a concentric disk," *Int. J. RF Microw. Comput. Aided Eng.*, Vol. 26, 268–276, 2016.